International Journal of Research Publication and Reviews

Journal homepage: www.ijrpr.com ISSN 2582-7421

Fe_2O_3 Modified ZnO Thick Film Resistors as H_2S Sensor

V. S. Kalyamwar[a]*, N. B. Thakare[b], S. D. Charpe[c], S. S. Kawar[d]

[a*] Department of Physics, Bharatiya Mahavidyalaya, Amravati,444605, India.
[b] Department of Physics, Shri Shivaji College of Arts, Commerce & Science, 444001, Akola, India.
[c] Department of Physics, J. D. Patil Sangludkar Mahavidyalaya, Daryapur Dist. Amravati, 444803, India.
[d] Department of Physics, Dr. R. G. Rathod Arts & Science College, Murtizapur Dist. Akola,444107, India.

Doi: https://doi.org/10.55248/gengpi.5.0724.1746

ABSTRACT :

Zinc oxide nanostructures were synthesized by chemical route method. The XRD spectrum indicates that the sample is wurtezite (hexagonal) structured ZnO with lattice constants of a = 3.249A^0, c = 5.206 A^0. Thick films of synthesized ZnO were prepared by screen printing technique. Fe_2O_3-modified ZnO thick films were obtained by dipping them into an aqueous solution of $FeCl_3$ for different intervals of time. Gas sensing properties of surface modified thick films were investigated. Fe_2O_3-modified ZnO thick film dipped for 1.5 min was observed to be more sensitive to H_2S as compared to other modified thick films at 200^{0}C. Effects of surface microstructure and CuO concentrations on the sensitivity, selectivity, response and recovery of the sensor in the presence of H_2S an other gases were studied and discussed.

Keywords: Fe2O3, Thick Films, H2S Sensor

Introduction :

Chemical sensors played important roles in industrial, medical and domestic applications in detecting pollutant, toxic and combustible gases. Key requirements for chemical sensors contain not only high sensitivity and good selectivity to a trace targeted gas, but also the abilities of working in a continuous mode at room temperature with fast response and easy recovery. One dimensional metal oxide nanostructures with a high surface to volume ratio have attracted much attention because their morphologies can be controlled and the surface can be simply modified [1-10].

Zinc oxide is an important oxide semiconductor for sensing applications [11-15]. Generally, ZnO sensors provide a wide variety of advantages, such as low cost, short response time, easy manufacturing and small size as compared to the traditional analytical instruments. However it has some drawbacks, such as high response and recovery time, poor gas selectivity and relatively low gas sensitivity.

To overcome these disadvantages, considerable research and development are underway. There are various techniques to modify the sensing properties of the gas sensors. One critical approach is to modify the metal oxide surface by using noble metals or rare earth metals [16-18].

In present study, efforts were made to prepare Fe_2O_3 activated ZnO nanostructure thick films and to study morphological, structural and sensing properties at room temperature.

2. Experimental

2.1. Synthesis of ZnO nanostructure

All chemicals were of analytical grade and were used as purchased without further purification. In present work, 4.461 gm Zn $(NO_3)_2{\cdot}6H_2O$ (Zinc nitrate hexahydrate) was dissolved in 100 ml distilled water and 2.0 g of NaOH was dissolved in 100 ml distilled water. The zinc nitrate solution was added drop wise to the NaOH solution to form white solution. Then, white solution was subsequently kept at 75 ^{0}C For 12 hr. The resulting white precipitates were collected by centrifugation, washed with distilled water and ethanol several times and then dried at 80^{0}C in vacuum oven for 2hr. Obtain ZnO nanostructure product were used for further study.

2.2. Preparation of thick films

Thick films of chemically synthesized ZnO nanostructure were prepared by using screen printing technique. In typical process, thixotropic paste was formulated by mixing the synthesized ZnO powder with ethyl cellulose (a temporary binder) in a mixture three of organic solvents namely butyl cellulose, butyl carbitol acetate and turpineol. The ratio of ZnO to ethyl cellulose was kept 95:05. The ratio of inorganic to organic part was kept as 75:25 in formulating the pastes. The thixotropic pastes were screen printed on a glass substrate in desired patterns. The films prepared were fired at 500^{0}C for 12hrs. Prepared thick films are termed as pure ZnO thick films.

2.3. Fe_2O_3 modified ZnO thick films

Surface of pure ZnO thick films were modified by dipping them into a 0.02 M aqueous solution of $FeCl_3$ for different intervals of time (0.5 min, 1 min 1.5 min and 2 min). After dipping, thick films were dried under IR lamp for 60 min. Dried thick films were calcinated at 500^0C for 2 hrs in air ambient. The $FeCl_3$ dispersed on the film surface was oxidized in calcination process, and sensor elements with different mass% of Fe_2O_3 on the surface of ZnO thick film were obtained. These surface activated films are termed as Fe_2O_3 modified films.

3. Materials characterization

3.1. X-ray diffraction studies

X-ray diffraction data for structural characterization of ZnO nanostructure synthesized by chemical route method was obtained on the Philips PW 1710 X-ray diffractometer using Cu-Kα source. X-ray diffraction pattern of synthesized ZnO nanostructure are helpful in studying the crystalline structure and determination of crystallite size.

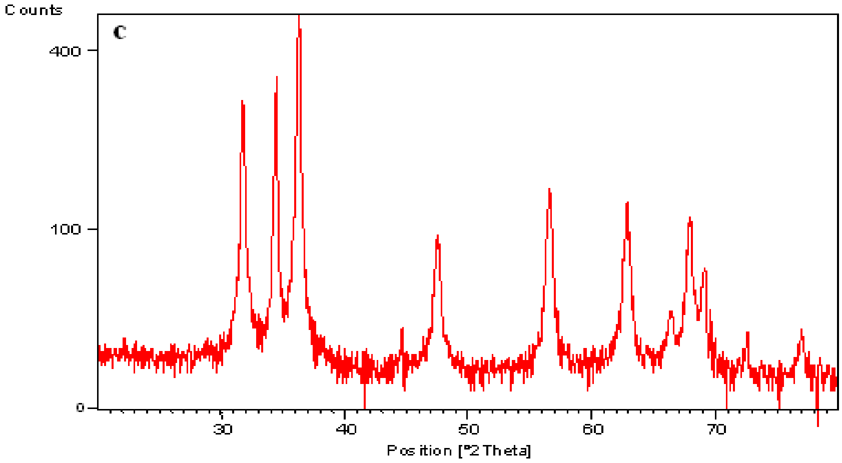

Fig. 1-powder XRD pattern of ZnO

The recorded XRD pattern (figure 1) confirmed that synthesized ZnO is high crystalline in nature. The corresponding X-ray diffraction peak for (100), (002), (101) and (102) planes confirm the formation of hexagonal wurtzite structure of ZnO, which are in good agreement with the literature values (JCPDS card No. 36-1451). In this XRD pattern, extra pick appear at $2\theta = 44^0$. This peak was identified as surface hydroxyl groups, which can be related to the formation of water on the ZnO nanostructure surface [19].

To extract more information on the crystallinity, the XRD data is exercised to determine the crystallite size. The full width at half maxima (FEHM) of the intense (101) peak was evaluated for all the ZnO nanostructures, by using Scherrer's formula [20].

$$D = \frac{K\lambda}{\beta\, sin\theta} \qquad (1)$$

Where λ is the wavelength of incident beam (1.5406 A^0), β is the FWHM of the peak in radians, θ is the diffraction angle and k is Scherrer constant. The average crystallite size calculated from (101) peak was approximately 16 nm.

3.2. Transmission electron microscope

Fig. 2- TEM image of ZnO

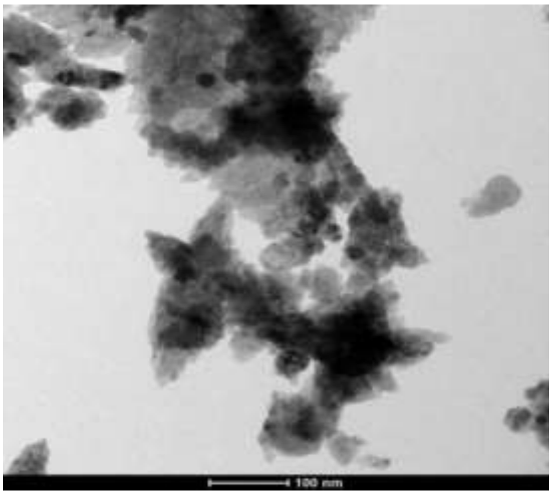

The morphology and particle size of ZnO sample synthesized by chemical route method were examined by using Techai G2 20 Ultra-Twin transmission electron microscope (Pune University, Pune). It is clearly seen form the TEM image that the large numbers of nanoparticles of ZnO were cumulative to form superior size crystal.

3.3. Scanning electron microscope

Figure 3a shows typical FE-SEM micrograph of the pure ZnO thick film prepared by screen printing technique. The ZnO synthesized by the chemical route method consist of randomly distributed hexagonal nanosheets.

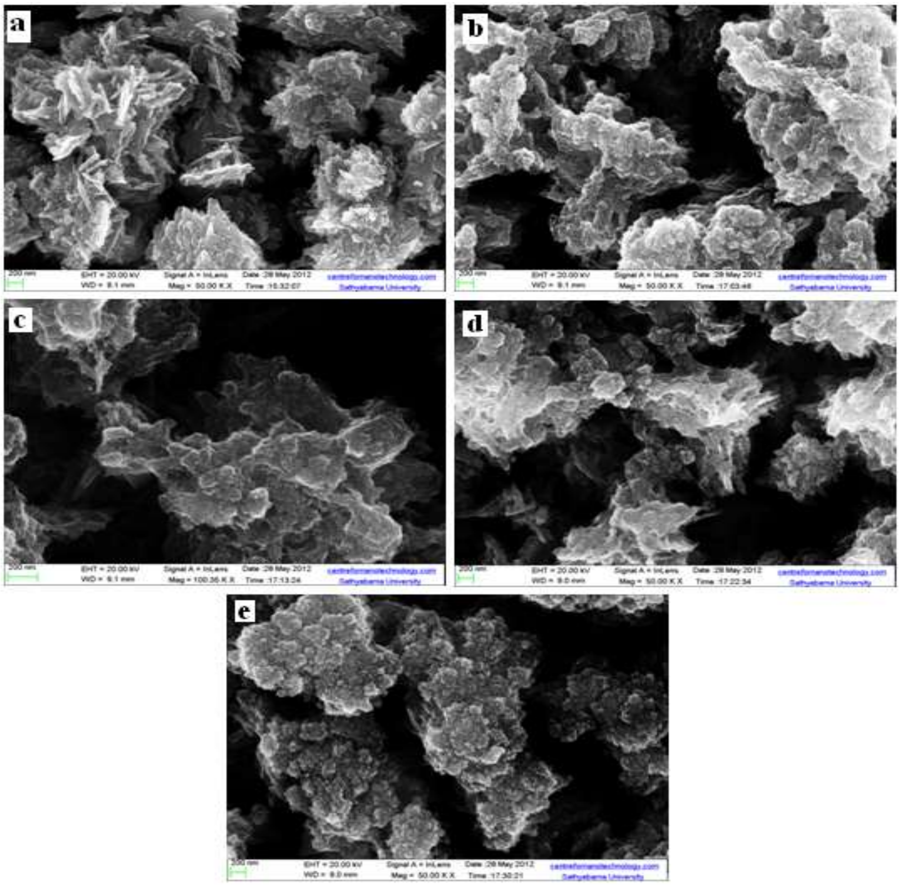

Fig.3- FE-SEM images of a) pure ZnO thick film b) Fe_2O_3 modified ZnO thick film (0.5 min dip.) c) Fe_2O_3 modified ZnO thick film (1 min dip.) d) Fe_2O_3 modified ZnO thick film (1.5 min dip.) e) Fe_2O_3 modified ZnO thick film (2 min dip.).

Figure 3b indicates that in the Fe_2O_3 modified ZnO thick film (0.5 min dipping), the Fe_2O_3 grain are randomly dispersed in the ZnO nanosheets. It shows that the grains of Fe_2O_3 consist of porous nature, cause increase in surface to volume ratio which is beneficial for gas sensing properties of the film.

The FE-SEM images in Figure 3b-3e clearly indicates that after the surface modification by dipping method, the growth of Fe_2O_3 grain began to occur on the surface of ZnO thick film. Figure 3b through 3e shows that as the dipping time increases, the more and more grain of Fe_2O_3 deposited over ZnO grain.

3.4. Elemental analysis

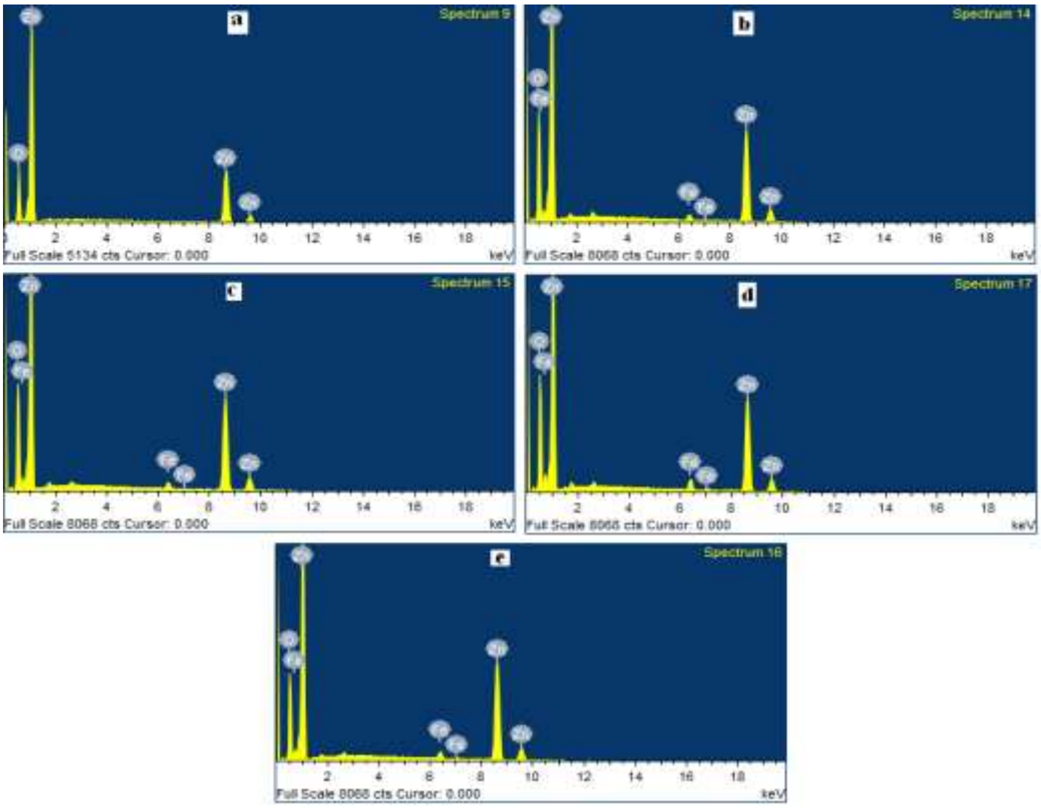

Fig. 4- EDS patterns of a) pure ZnO thick film b) Fe_2O_3 modified ZnO thick film (0.5 min dip.) c) Fe_2O_3 modified ZnO thick film (4 min dip.) d) Fe_2O_3 modified ZnO thick film (6 min dip.) e) Fe_2O_3 modified ZnO thick film (8 min dip.).

The quantitative elemental composition of the pure and Fe_2O_3 modified ZnO thick films were analyzed using an Energy Dispersive Spectrometer. Figure 4 represent the EDS pattern of pure and Fe_2O_3 modified ZnO Thick films. The mass % of Zn, O and Fe elements in pure and modified thick films is represented in Table 1.

Table 1- Mass % of Zn, O and Fe elements in pure and modified thick films

Sample	**Pure ZnO**	**Fe_2O_3 modified ZnO thick film (with different dipping time)**			
Element		**0.5 min**	**1 min**	**1.5 min**	**2 min**
O	25.63	26.53	25.65	26.77	23.94
Zn	74.37	72.00	72.59	70.43	73.11
Fe	00	1.47	1.79	2.80	2.95

In zinc oxide, standard stoichiometric mass percentage of zinc and oxygen are 80.347 and 19.653 respectively. Results of EDS show that the mass percentages of Zn and O in each film were not as per the stoichiometric ratio. Table 1 reveals that all films were observed to be the oxygen rich. Non-stoichiometric ratio of the constituent element leads the semiconducting nature of the material. Form table it is also clear that, as the dipping time increases the mass % of Fe increases.

4. Results and discussion

Gas sensing properties of Fe_2O_3 modified ZnO thick films

4.1. Gas response

The gas response of Fe_2O_3 modified ZnO thick films to 30 ppm H_2S were investigated at various operating temperatures ranging from room temperature to 300^0C. The gas response of Fe_2O_3 modified ZnO thick films as a function of operating temperature is shown in figure 5. This figure shows that, the sensitivity of 1.5 min dipped Fe_2O_3 modified ZnO thick film is highest among other thick films at operating temperature 200^0C.

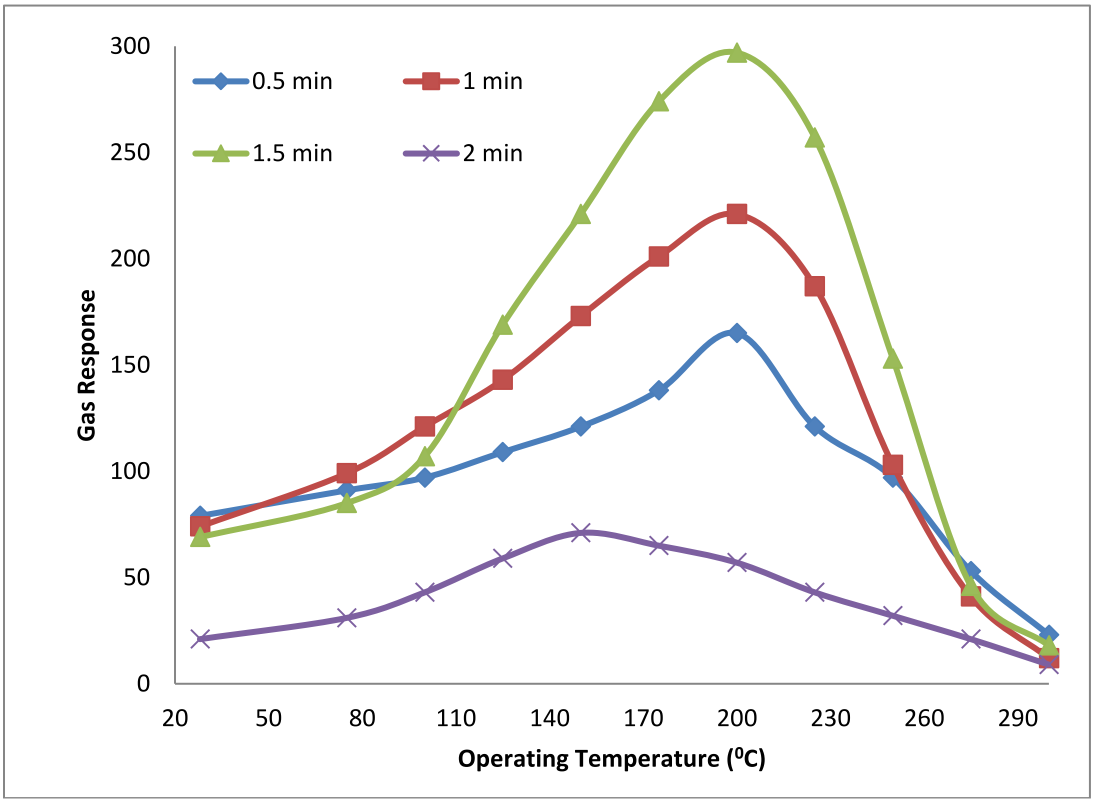

Fig. 5- variation of gas response of Fe_2O_3 modified ZnO thick films with operating temperature.

4.2. Selectivity

Figure 6 illustrates the selectivity of all Fe_2O_3 modified ZnO thick films for 30 ppm H_2S gas at room temperature. These modified thick films showed high selectivity towards low concentration (30ppm) H_2S among all the gases such as CO_2, NH_3 and LPG.

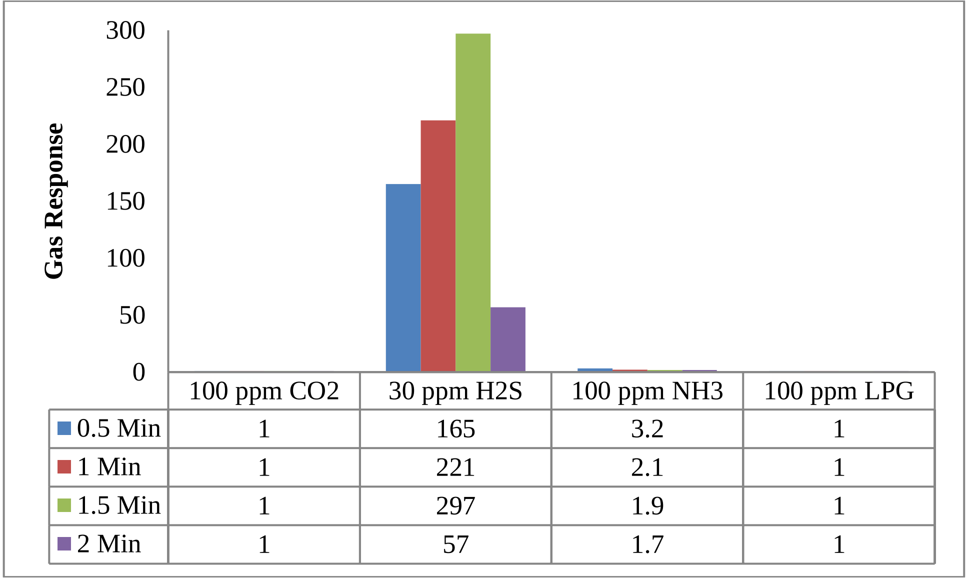

	100 ppm CO2	30 ppm H2S	100 ppm NH3	100 ppm LPG
■ 0.5 Min	1	165	3.2	1
■ 1 Min	1	221	2.1	1
■ 1.5 Min	1	297	1.9	1
■ 2 Min	1	57	1.7	1

Fig. 6- Comparison of gas response of Fe_2O_3 modified ZnO thick film (1.5 min dip.) to different gases at 200^0C.

4.3. Response and recovery

Response and recovery times are basic parameters of the gas sensors. Response and recovery time of all modified thick films at 200^0C for 30ppm H_2S were examined and summarize in table 2.

Table 2- The response and recovery time of Fe_2O_3 modified ZnO thick films at 200^0C

Fe_2O_3 modified ZnO Thick film (different dipping time)	**Response time (s)**	**Recovery time (s)**
0.5 min	120	234
1 min	30	78
1.5 min	6	45
2 min	5	33

The response and recovery time of (1.5 min) Fe_2O_3 modified ZnO thick film at 200^0C was found 6s and 45s respectively i.e. the 90% response and recovery were attained within 6s and 45s respectively.

The study of gas sensing properties of the Fe_2O_3 modified ZnO thick films shows that the gas sensing properties is greatly influenced by the operating temperature. Figure 5 it can be seen that Fe_2O_3 modified ZnO thick films are sensitive to low concentration (30 ppm) H_2S at room temperature. When the temperature is in the range 180^0C to 200^0C, the highest sensitivity of thick films was obtained. Higher sensitivity of these thick films at 200^0C may be due to following two reasons.

When H_2S adsorb between the grains of Fe_2O_3 and ZnO, the potential barrier would be decreased as a results of oxidative conversion of the H_2S gas and desorption of oxygen. Due to desorption of adsorbed oxygen ions and conversion of zinc oxide into zinc sulfates the resistance of the film would decreases sharply leading to high response to H_2S.

For metal oxide semiconductor based sensors, the change in resistance is mainly caused by the adsorption and desorption of oxygen on the surface of sensing materials. The oxygen species capture electrons from the materials, which results in the concentration changes of electrons in Fe_2O_3 modified ZnO sensor. When the sensor is exposed to H_2S, the reductive gas reacts with the oxygen adsorbed on the sensor surface and the electrons are released back into the semiconductor, resulting in the increased in electrical conductance of the Fe_2O_3 modified ZnO sensor. This reaction can be expressed as follows

$H_2S + 3O_2 \rightarrow H_2O + SO_2 + 6e^-$

For the Fe_2O_3 modified ZnO thick films, the low response at low operating temperature can be attributed to the low thermal energy of the gas molecules, which is not enough to react with the surface adsorbed oxygen species. As a result, the reaction rate between them is essentially low and low response is observed.

5. Conclusions :

The sensing performance of pure and Fe_2O_3 modified ZnO thick films can be summarized as:Zinc oxide powder synthesized by chemical route method consists of nanoparticles and nanorods with average crystallite size 16 nm. All Fe_2O_3 modified ZnO thick films shows sensitive to low concentration of H_2S at room temperature. All Fe_2O_3 modified ZnO thick films were observed to be higher selective to 30 ppm H_2S gas from other test gases of higher concentrations. At 200^0C, Fe_2O_3 modified ZnO thick film (1.5 min dipping) shows higher sensitivity to 30 ppm of H_2S as compared to other Fe_2O_3 modified ZnO thick films.

REFERENCES :

1. Zhang Y., He X.L., Li J.P., Miao Z.J., Huang F., Sensors and Actuators B 132 (2008) 67–73.
2. Si S.F., Li C.H., Wang X., Peng Q., Li Y.D., Sensors and Actuators B 119 (2006) 52–56.
3. Xua P.C., Cheng Z.X., Pan Q.Y., Xu J.Q., Xiang Q., Yu W.J., Chu Y.L., Sensors and Actuators B 130 (2008) 802–808.
4. Hsueh T.J., Hsu C.L., Chang S.J., Chen I.-C., Sensors and Actuators B 126 (2007) 473–477.
5. Chen Y.J., Xue X.Y., Wang Y.G., Wang T.H., Applied Physics Letters 87 (2005) 233503-233503.
6. Kaur M., Jain N., Sharma K., Bhattacharya S., Roy M., Tyagi A.K., Gupta S.K., Yakhmi J.V., Sensors and Actuators B 133 (2008) 456–461.
7. Chen Y.J., Zhu C.L., Xiao G., Sensors and Actuators B 129 (2008) 639–642.
8. Wang C.H., Chu X.F., Wu M.M., Sensors and Actuators B 113 (2006) 320–323.
9. Chen Y.J., Zhu C.L., Xiao G., Sensors and Actuators B 129 (2008) 639–642.
10. Wan Q., Li Q.H., Chen Y.J., Wang T.H., He X.L., Li J.P., Lin C.L., Applied Physics Letters 84 (2004) 3654–3656.
11. Jones A., Jones T.A., Mann B., Griffith J.G., Sensors and Actuators 5 (1984) 75–88.
12. Pizzini S., Butta N., Norducci D., Palladino M., Journal of electrochemical society of India 136 (1989) 1945–1948.
13. Nanto H., Minami T., Takata S., Journal of Applied Physics 60 (1986) 482–484.
14. Basu S., Dutta A., Sensors and Actuators B 22 (1994) 83–87.

15. Lou X., Journal of Sensors Trans. Technologies 3 (1991) 1–5.
16. Boccizzi F., Chiorino A., Tsubota S., Haruta M., Sensors and Actuators B 24–25 (1995) 540–543.
17. Bhooloka Rao B., Chemical Physics 64 (2000) 62–65.
18. Gentry S.J., Jones T.A., Sensors and Actuators B 10 (1986) 141–163.
19. Kester W J Wong, Matthew R Field, Jian Zhen Ou, Kay Latham, Michelle J S Spencer, Irene Yarovsky, Kourosh Kalantar-zadeh, *Nanotechnology* 23 (2012) 015705
20. Hilber, T.; Letonja, P.; Marr, R.; Poit, P.; Siebenhofer, M. Part. Part. Syst. Charact. 2002, 19, 342-347.